Life Sciences 237 (2019) 116769

Contents lists available at ScienceDirect

Life Sciences

journal homepage: www.elsevier.com/locate/lifescie

LncRNA Tug1 involves in the pulmonary vascular remodeling in mice with hypoxic pulmonary hypertension *via* the microRNA-374c-mediated Foxc1

Lei Yang[a,*], Huan Liang[b], Li Shen[c], Zhanjiang Guan[a], Xianguo Meng[a]

[a] ICU, The Third Affiliated Hospital of Qiqihar Medical University, Qiqihar 161002, PR China
[b] Department of Urology Surgery, The Third Affiliated Hospital of Qiqihar Medical University, Qiqihar 161002, PR China
[c] Glorious Community, The Third Affiliated Hospital of Qiqihar Medical University, Qiqihar 161002, PR China

ARTICLE INFO

Keywords:
Long noncoding RNA Tug1
MicroRNA-374c
Foxc1
Hypoxic pulmonary hypertension
Proliferation
Apoptosis
Migration
Pulmonary vascular remodeling
NOTCH signaling pathway

ABSTRACT

Hypoxic pulmonary hypertension (HPH) is a serious and potentially devastating disorder of the pulmonary circulation with complicated mechanisms. Long non-coding RNA (lncRNA) has been revealed to participate in HPH development. This study aimed to explore how lncRNA Tug1 affected the pulmonary vascular remodeling in HPH. A mouse model of HPH and a pulmonary artery smooth muscle cell (PASMC) model of HPH (HPH-PASMCs) were established, where the expression of lncRNA Tug1 was determined. Then, the interaction among lncRNA Tug1, miR-374c, and Foxc1 was assessed. Finally, in order to determine the effects of lncRNA Tug1 on PASMC activities and pulmonary vascular remodeling after HPH, the expression of lncRNA Tug1 was silenced in HPH-PASMCs and HPH mice, with the proliferation, apoptosis, and migration of PASMCs as well as blood pressure in mice measured, respectively. The obtained data revealed that lncRNA Tug1 was highly expressed in HPH mice and HPH-PASMCs. In addition, lncRNA Tug1 up-regulated the expression of Foxc1 by binding to miR-374c. Notably, silencing of lncRNA Tug1 inhibited the proliferation and migration, but promoted the apoptosis of PASMCs. Moreover, lncRNA Tug1 silencing was observed to attenuate the pulmonary vascular remodeling in HPH mice through the Foxc1-mediated NOTCH signaling pathway. Taken conjointly, silencing of lncRNA Tug1 down-regulated the Foxc1 expression by binding to miR-374c, thereby inhibiting the proliferation and migration, while promoting apoptosis of PASMCs to impede pulmonary vascular remodeling in HPH *via* the Notch signaling pathway. This study provided novel therapeutic insights for treating HPH.

1. Introduction

Clinical manifestations associated with pulmonary hypertension (PH) are non-specific and versatile, such as exertional dyspnea, tiredness, weakness, light-headedness or syncope, chest pain, cough, with the possibility of progressing into right-sided heart failure in a more accelerated disease [1,2]. Hypoxic pulmonary hypertension (HPH), a type of PH, is characterized by constantly elevated arterial pressure caused by low oxygen levels in pulmonary blood [3]. It is widely accepted that hypoxic conditions trigger pulmonary vasoconstriction and vascular remodeling, as well as causing inflammation and damage to the blood vessels in the lungs [4]. However, HPH development deals profoundly with various blood cell types as well as different types of cytokines and chemokines that participate in the process [5]. Recently, new and upcoming studies have that uncovered gene deficiency is a driver of HPH progression [6], especially noncoding RNAs [7].

Long noncoding RNAs (lncRNAs), transcripts longer than 200 nt, lack the ability of protein-coding and exert their function on the form of RNA [8]. The results of a previous RNA profiling analysis revealed that 2004 lncRNAs are up-regulated and 507 lncRNAs are down-regulated, whereas 609 mRNAs are highly expressed and 560 mRNAs are poorly expressed in idiopathic PH [9], highlighting the heavy involvement of lncRNAs and mRNAs in HPH pathogenesis. Meanwhile, several microRNAs (miRNAs) have also been discovered to regulate HPH vascular remodeling [10]. Additionally, the microarray analysis of the current study identified a highly expressed taurine up-regulated gene1 (Tug1) in HP, and predicted that lncRNA Tug1 possesses the potential to bind to miR-374c to regulate forkhead box C1 (Foxc1). Tug1, over-expressed in various human cancers (except non-small cell lung cancer and multiple myeloma), is a novel oncogene that promotes cancer cell proliferation, invasion, and migration at least partially by means of chromatin remodeling and sequestration of miRNAs [11]. In addition, miR-

* Corresponding author at: ICU, The Third Affiliated Hospital of Qiqihar Medical University, No. 27, Taishun Street, Qiqihar 161002, Heilongjiang Province, PR China.
E-mail address: yang_lei2019@163.com (L. Yang).

https://doi.org/10.1016/j.lfs.2019.116769
Received 3 April 2019; Received in revised form 12 August 2019; Accepted 13 August 2019
Available online 15 August 2019

374c-5p up-regulation has been proven to effectively suppress cervical cancer cell invasion and migration through inhibition of its target gene, Foxc1 [12]. Specifically, silencing of the Foxc1 expression in specific cell types provides novel insights into the development of vessels in normal growth or vessels under pathological conditions [13]. Moreover, the hypoxia-regulated NOTCH signaling pathway also affects the progression of pulmonary vascular remodeling in HPH through functional activation and up-regulation of CaSR [14]. The NOTCH pathway is also implicated with the cell behavior mechanism which is regulated by various miRNAs such as miR-34a and miR-9 [15,16]. Therefore, the current study aims to investigate the regulation of lncRNA Tug1 in the pathogenesis of HPH, with the involvement of the miR-374c/Foxc1/NOTCH axis.

2. Materials and methods

2.1. Ethics statement

The current study was approved by the Animal Ethics Committee of The Third Affiliated Hospital of Qiqihar Medical University. Animal use and experimental procedures were conducted in accordance with the Guide for the Care and Use of Laboratory Animals published by the National Institutes of Health, and all efforts were made to minimize the number and suffering of the included animals.

2.2. Establishment of HPH mouse model

A total of 40 adult male healthy C57BL/6 mice (weighing 14–25 g) were purchased from the Experimental Animal Center of Harbin Medical University (Heilongjiang, China). Among the included mice, 10 mice were maintained in normal circumstances as the normal control, and the remaining 30 were subjected to hypoxia conditions (12% O_2) for 9 days to establish HPH models. Furthermore, 5 normal mice and 15 HPH mice were anaesthetized by intraperitoneal injection with 50 mg/kg pentobarbital sodium. After complete anesthesia, the mice were incised open to obtain heart and lung specimens. The obtained hearts and lungs were placed in cold phosphate buffer sodium (PBS) and used for subsequent experimentation.

2.3. Pulmonary artery smooth muscle cell (PASMC) isolation and cell treatment

Distal pulmonary artery smooth muscle tissues were isolated from the C57BL/6 mice under a stereo microscope. The separated tissues were disinfected with ultraviolet radiation for 15 min and then washed with calcium-free hank's balanced salt solution (HBSS) (H6648, Sigma-Aldrich Chemicals, Deisenhofen, Germany). Next, the tissues were detached for 7–8 min at 37 °C using the mixed enzyme digestion of collagenase type I and papain (1:1) which was dissolved in Dulbecco's modified eagle medium (DMEM). Then, 1 mL of medium containing 20% fetal bovine serum (FBS) (10100147, Gibco BRL/Invitrogen Inc., CA, USA) was added to the detached tissues to terminate the detachment process. Subsequently, the tissues were centrifuged at 1000 r/min for 2 min and made into a cell suspension with the addition of DMEM low glucose medium (D6046, Sigma-Aldrich Chemicals, Deisenhofen, Germany) containing 20% FBS. The cell suspension was then seeded into a 35 mm culture dish with coverslip for 30 min at room temperature. Finally, the cells adhering to the wall were identified and cultured with medium with 5% CO_2 at 37 °C.

For cell grouping, isolated PASMCs were transfected with the plasmids and grouped into short interfering RNA (sh)-NC, sh-Tug1, sh-NC + over-expression (oe)-NC, sh-NC + oe-Foxc1, sh-Tug1 + oe-NC, sh-Tug1 + oe-Foxc1, mimic NC, miR-374c mimic, inhibitor NC, and miR-374c inhibitor groups.

For *in vivo* treatment, the mice were grouped by carrying out injection with the PASMCs after transfection of both sh-NC and oe-NC, both sh-Tug1 and oe-NC, as well as both sh-Tug1 and oe-Foxc1 plasmids (n = 5) [17]. In brief, 12.5 μg of nucleic acid was firstly diluted to a concentration of 1 μg/μL with endotoxin-free pure water. A final volume of 50 μL was reached by supplementing 12.5 μL of water and 10 μL of 10% glucose solution (w/v). Next, a total of 25 μL of 10% glucose solution was added to 25 μL of entranster™-*in vivo* animal transfection reagent (18668-11-1, Engreen, Beijing, China) for a final volume of 50 μL. The diluted transfection reagent was immediately mixed with the diluted nucleic acid solution and allowed to stand for 15 min. Afterwards, the transfection reagent was injected into the mice *via* the tail vein at distal end of 1/3. A total of 100 μg of nucleic acid and 50 μL of transfection reagent were employed for this portion of the experiment.

The isolated PASMCs were routinely cultured in smooth muscle cell growth medium-2 (SmGM-2™) supplemented with 5% FBS (S00725, Gibco BRL/Invitrogen Inc., Carlsbad, CA, USA) and penicillin/streptomycin (100 units/mL of medium; 15140122, Gibco BRL/Invitrogen Inc., Carlsbad, CA, USA). Next, the PASMCs were cultured in an anoxic chamber (3%O_2, 5%CO_2) for 48 consecutive h, and ultimately passaged to the 3rd generation for subsequent experiments. In addition, HEK-293T cells purchased from American Type Culture Collection (Manassas, VA, USA) (https://www.atcc.org/) were cultured in DMEM containing 10% FBS (10100147, Gibco BRL/Invitrogen Inc., CA, USA) supplemented with penicillin/streptomycin (100 units/mL of medium) under normoxia conditions with 5% CO_2 in air at 37 °C.

2.4. RNA fluorescence in situ hybridization (FISH)

The localization of lncRNA Tug1 in mice PASMCs was identified using a FISH assay in strict accordance with the instructions of Ribo™ lncRNA FISH Probe Mix (Red) Kit (Guangzhou RiboBio Co., Ltd., Guangdong, China). Firstly, cover slips were placed in a 24-well plate, followed by the cells being seeded in a 24-well plate at the density of 6×10^4 cells/well. Once cell confluence reached approximately 85%, the cells were fixed in 1 mL of 4% paraformaldehyde solution at room temperature and added with 250 μL of prehybridization overnight after being treated with proteinase K (2 μg/mL) (Beijing Solarbio Science & Technology co. ltd., Beijing, China), glycine, and an acetolylation reagent. Next, the cells were stained in a 24-well culture plate for 5 min with 4′-6-diamidino-2-phenylindole (DAPI), which was diluted using a phosphate buffer saline-Tween 20 (PBST) (800:1). Finally, the cells were mounted with an anti-fluorescent quencher, observed, and photographed under a fluorescence microscope (Olympus Optical Co., Ltd., Tokyo, Japan) with 5 random visual fields.

2.5. RNA-binding protein immunoprecipitation (RIP)

A RIP kit (Millipore Corp of Billerica, Massachusetts, USA) was applied to detect the binding of Ago2 to lncRNA Tug1, miR-374c, and Foxc1, in mouse PASMCs. Firstly, the cells were rinsed with pre-cooled PBS, followed by lysis with equal volume of radio-immunoprecipitation assay (RIPA) lysate (P0013B, Beyotime Biotechnology Co., Jiangsu, China) for 5 min. The supernatant was then collected after being centrifuged at 14,000 rpm for 10 min at 4 °C. Subsequently, a portion of the cell extract was removed as the input, while the remaining portion was incubated with the antibody for co-precipitation. The specific steps were as follows: 50 μL of magnetic beads collected from every co-precipitation reaction system were washed and resuspended using 100 μL RIP wash buffer, with the addition of 5 μg of antibody for binding based on grouping. Next, the magnetic bead-antibody complex was resuspended in 900 μL of RIP wash buffer and incubated overnight with 100 μL of the cell extract at 4 °C. After incubation, the magnetic bead-protein complex was collected on a magnetic base. The sample and input were detached using protease K to extract total RNA content for subsequent reverse transcription quantitative polymerase chain reaction (RT-qPCR). The antibodies employed for RIP were Ago2 (ab32381, dilution ratio of 1:1000, Abcam, Cambridge, UK) (mixed at room

temperature for 30 consecutive min), and immunoglobulin G (IgG) (ab109489, dilution ratio of 1:100, Abcam, Cambridge, UK) (serving as the negative control). Finally, the expression of lncRNA Tug1, miR-374c and Foxc1 in mouse PASMCs was examined using RT-qPCR.

2.6. Dual luciferase reporter gene assay

Bioinformatics were applied to analyze the binding relationship among miR-374c, lncRNA Tug1 and Foxc1, the results of which were verified by dual luciferase reporter gene assay. Firstly, artificially synthesized lncRNA Tug1 and 3'untranslated region (3'UTR) of Foxc1 mRNA were introduced into the pMIR-reporter (Huayueyang Biotechnology Co., Ltd. Beijing, China) with the use of endonuclease sites, *Spe*I and Hind III. Then, the complementary sequence mutation sites of the seed sequences were designed respectively on the wild type (wt) of Tug1 and Foxc1, with the target fragments being inserted into the pMIR-reporter plasmid using T4 DNA ligase post restriction endonuclease digestion. Next, HEK-293T cells were cultured in DMEM with 10% FBS and penicillin/streptomycin (100 units/mL of medium) with 5% CO_2 in air at 37 °C. The correctly sequenced luciferase reporter plasmids WT and mutant (MUT), together with lncRNA Tug1 and miR-374c, were co-transfected with HEK-293T cells (Cell Bank of Shanghai Institutes for Biological Sciences, Chinese Academy of Sciences, Shanghai, China). Subsequently, the cells were collected and lysed 48 h after transfection; the luciferase activity was assessed using luciferase assay kits (K801-200, Biovision Research Products, Mountain View, CA) by a fluorescence detector Glomax20/20 luminometer (Promega Corporation, Madison, WI, USA).

2.7. RNA extraction and quantification

Total RNA content in PASMCs was extracted following guidelines provided by the RNeasy Mini Kit (Qiagen, Valencia, CA, USA) and reverse transcribed into complementary DNA (cDNA) using reverse transcription kits (RR047A, Takara Bio Inc., Otsu, Shiga, Japan). The samples were then subjected to RT-qPCR using SYBR Premix EX Taq kits (RR420A, Takara Bio Inc., Otsu, Shiga, Japan) on a real-time PCR instrument (ABI7500, ABI, Foster City, CA, USA). Three replicate wells were set for each sample. All primers were synthesized by Sangon Biotechnology Co. Ltd. (Shanghai, China) (Table 1). By using glyceraldehyde 3-phosphate dehydrogenase (GAPDH) or U6 as the internal reference for lncRNA gene or microRNA gene, the fold changes between the experimental and control group were calculated using means of relative quantification (the $2^{-\Delta\Delta Ct}$ method).

2.8. Western blot analysis

Total protein content in tissues or cells was extracted using RIPA lysis buffer containing phenyl-methyl-sulphonyl fluoride (PMSF). Next, the extracted proteins were separated with sodium dodecyl sulfate-polyacrylamide gel electrophoresis (SDS-PAGE) and transferred onto the polyvinylidene fluoride (PVDF) membrane. The membrane was then blocked with 5% skim milk powder at room temperature for 1 h. Afterwards, the membrane was incubated overnight at 4 °C with the following primary rabbit antibodies specific for Bcl2-Associated X (Bax) (ab182733, dilution ratio of 1:1000), Ki-67 (ab16667, dilution ratio of 1:1000), Matrix metalloprotease (MMP)-2 (ab37150, dilution ratio of 1:1000), MMP-9 (ab228402, dilution ratio of 1:1000), hypoxia inducible factor (HIF)-α (ab2185, dilution ratio of 1:1000), vascular endothelial growth factor (VEGF) (ab32152, dilution ratio of 1:1000), NOTCH1 (ab8925, dilution ratio of 1:500), NOTCH3 (ab23426, dilution ratio of 1:1000), and GAPDH (ab9485, dilution ratio of 1:2500). After rinsing with tris-buffered saline tween (TBST) (10 min each time) 3 times, the membrane was incubated with the horseradish peroxidase (HRP)-labeled goat anti-rabbit IgG H&L secondary antibody (ab6721, dilution ratio of 1:2000) for 1 h. All the aforementioned antibodies were purchased from Abcam Inc. (Cambridge, UK). Subsequently, the membrane was developed with an enhanced chemiluminescence (ECL) reagent (BB-3501, Bestbio, Shanghai, China) and exposed using a gel imager. Finally, the results were photographed with the Bio-Rad image analysis system (Bio-Rad, Inc., Hercules, CA, USA) and analyzed with the Quantity One v4.6.2 software. The relative protein expression was expressed as the gray value ratio of protein bands to GAPDH.

2.9. Cell counting kit-8 (CCK-8)

The cells were seeded in a 96-well plate at a density of 2×10^3 cells/well, and a blank control group only added with medium without cells was regarded as the zero setting. Then, 24 h after transfection, cells in each well were added with 10 μL CCK-8 solution respectively at 0, 24, 48, 72, and 9 h. After addition, the cells were then incubated for 4 h at 37 °C. Absorbance at 450 nm was measured using a microplate reader (Bio-Rad, Inc., Hercules, CA, USA). The ratio of the absorbance of the experimental groups to the control group was calculated in order to plot the cell viability curve.

2.10. Flow cytometry

Following transfection, cells in each group were detached using 0.25% trypsin solution, which was terminated with the addition of RPMI-1640 medium containing 10% FBS. Next, the cells were centrifuged for 5 min at 1000 r/min and fixed with precooled 70% ethanol at 4 °C. Subsequently, after the cell concentration was adjusted to 1×10^6 cells/mL, the cells were stained with 10 mL Annexin V-fluorescein isothiocyanate (FITC)/propidiumiodide (PI) (556547, Shuojia Biotechnology Co., Ltd., Shanghai, China) at 4 °C for approximately 15–30 min. Then, cell apoptosis was detected using a flow cytometer (Beckman Coulter, USA) to measure FITC at excitation wavelength of 480 nm and 530 nm and PI at the excitation wavelength of over 575 nm.

Table 1
Primer sequences for RT-qPCR.

Genes	Primer sequence
Tug1	Forward: 5′- GAGACACGACTCACCAAGCA-3′
	Reverse: 5′- GAAGGTCATTGGCAGGTCCA-3′
miR-374c	Forward: 5′- GGGGAUAAUACAACCUGCUAAGUGCUAGAACACUUAGCAGGUUGUA-3′
	Reverse: 5′- CAGTGCGTGTCGTGGAGT-3′
foxc1	Forward: 5′- AAATGTGGAGAAAACTTCTAGGTG-3′
	Reverse: 5′- ACTGTGGTAACACTGGTGCTGA-3′
GAPDH	Forward: 5′- GTTGTCTCCTGCGACTTCA-3′
	Reverse: 5′- TGGTCCAGGGTTTCTTACTC-3′
U6	Forward: 5′- TCCGACGCCGCCATCTCTA-3′
	Reverse: 5′- TATCGCACATTAAGCCTCTA-3′

Note: RT-qPCR, reverse transcription quantitative polymerase chain reaction; miR-374c, microRNA-374c; GAPDH, glyceraldehyde 3-phosphate dehydrogenase.

2.11. Transwell assay

Matrigel (40111ES08, Yeasen Company, Shanghai, China) diluted with pre-cooled serum-free DMEM (Matrigel:DMEM = 1:8) was added to the apical chamber of the Transwell chamber (3413, Beijing Unique Biotechnology Co., Ltd., Beijing, China). Next, the cells were cultured in an incubator at 37 °C for 4–5 h until solidification, made into cell suspension (1×10^6 cells/well) with 100 μL serum-free medium, and seeded into the apical chamber. A total of 500 μL DMEM medium containing 20% FBS was added to the basolateral chamber, and 3 replicate wells were set for individual groups. After incubation for 24 h at 37 °C with 5% CO_2, the cells were fixed with 5% glutaraldehyde at 4 °C and stained for 5 min using 0.1% crystal violet. Cells on the surface were removed using cotton swabs, and the remaining cells were observed under an inverted fluorescence microscope (TE2000, Nikon Corporation, China). With 5 visual fields randomly selected, cells were photographed (200×) and cells passing through the chamber were counted with the mean value calculated.

2.12. Blood pressure measurement

A blood pressure measuring catheter was connected to an electrocardiogram (ECG) monitor (G3N, Zetian Information Technology Co., Ltd., Beijing, China) *via* a pressure transducer (YPJ01, Jinyang Wanda Technology Co., Ltd., Beijing, China). The catheter was then slowly inserted from the right external jugular vein after dissection. The right ventricular systolic pressure (RVSP) and mean pulmonary artery pressure (mPAP) were recorded in real time upon stabilization of pressure waveform. After right heart catheterization pressure was measured, blood samples were collected from the left common carotid artery and centrifuged at 1500 r/min for 10 consecutive min to collect the plasma. Simultaneously, the heart was removed at once, and the right ventricle and left ventricle and ventricular septum were disjointed. Finally, the right ventricle (RV) and left ventricle + ventricular septum (LV + S) were weighed, and the right ventricular hypertrophy index (RVHI) was expressed as RV / (LV + S). Right ventricular mass changes were assessed with RVHI and RV/BW.

2.13. Hematoxylin and eosin (HE) staining

Pulmonary artery tissues were fixed in 4% paraformaldehyde solution at 4 °C for 48 consecutive h, and then stored in 0.02% azide solution. The pulmonary artery tissues were then dehydrated with gradient alcohol solution (70%, 80%, 90%, 95%, and 100%), immersed in absolute alcohol, treated using isobutyl alcohol and n-butanol, embedded with paraffin, and finally sectioned. The sections were dewaxed, cleared using xylene, and hydrated with gradient alcohol. Then, the sections were stained with hematoxylin for 20 min and differentiated with 0.5% hydrochloric acid solution for 10–30 s to terminate staining. After returning to blue coloration under tap water, the sections were counterstained with 0.5% eosin for 2 min, which was terminated by 95% ethanol rinse. Subsequently, the sections were baked at 57 °C, dehydrated with absolute ethanol (5 min, 2 times), cleared using xylene (5 min, 2 times), and mounted with neutral balsam. The structure of pulmonary vascular tissues was observed using an optical microscope.

2.14. Statistical analysis

Statistical analyses were performed using the SPSS 21.0 (IBM SPSS Statistics, Chicago, IL, USA). Measurement data were expressed as mean ± standard deviation. Unpaired *t*-test was used for comparing data in an unpaired design between two groups that conformed to the normal distribution and the homogeneity of variance. One-way analysis of variance (ANOVA) was used for data comparison among multiple groups, and repeated measures ANOVA was used for data comparison among multiple groups at different time points, followed by Tukey's *post hoc* test. Pearson's correlation was used to analyze the correlation between indicators and the difference was regarded as statistically significant when $p < 0.05$.

3. Results

3.1. LncRNA Tug1 is highly expressed in HPH mice

Analysis of the gene expression dataset GSE2411 using the Gene Expression Omnibus (GEO) database revealed that lncRNA Tug1 expression was up-regulated in HPH (Fig. 1A). Subsequently, HPH mouse model was established to validate the expression of Tug1 in HPH. Blood pressure measurement and analyses revealed that RVSP, RV, the wet weight ratio of RV to LV + s, and the right ventricular pressure (RVP) were significantly elevated in the HPH group in comparison with the normal group ($p < 0.05$). Additionally, HE staining results demonstrated that the pulmonary artery wall (PAW) was thicker in the model mice with HPH than normal mice (Supplementary Fig. 1). These findings confirmed the successful establishment of HPH mouse models. Furthermore, RT-qPCR was employed to determine the expression of lncRNA Tug1 in the pulmonary artery smooth muscle tissues of HPH mice (Fig. 1B) and HPH-PASMCs (Fig. 1C), which revealed elevated expression of lncRNA Tug1 in pulmonary artery smooth muscle tissues of HPH mice and HPH-PASMCs.

3.2. LncRNA Tug1 silencing inhibits proliferation and migration, while promoting apoptosis of PASMCs

PASMCs are the major cell type found in the intravascular wall of pulmonary arteries, making them suitable for examining the physiological functions of pulmonary arteries under various conditions. PASMCs were isolated and hypoxia mouse models were established as previous reported. Moreover, the above findings demonstrated that lncRNA Tug1 was highly expressed in HPH mouse tissues. In order to further investigate the effects of lncRNA Tug1 on the biological characteristics of HPH mice, the influence that lncRNA Tug1 had on PASMCs of mice was explored through *in vitro* experimentation. PASMC isolation and HPH mice model establishment were described as above. In the current study, lncRNA Tug1 silencing was observed in PASMCs under hypoxic conditions. Then, the effects of lncRNA Tug1 silencing on the proliferation, apoptosis, and migration of HPH-PASMCs were evaluated by determining the levels of corresponding marker proteins such as nuclear factor proliferating cell nuclear antigen (PCNA) protein, proliferation- and apoptosis-related protein Ki-67, Bax as well as migration-related proteins MMP-2, and MMP-9. Additionally, RT-qPCR (Fig. 2A) was employed to assess the cell silencing efficiency of PASMCs in individual groups. These results demonstrated significantly decreased lncRNA Tug1 expression in the sh-Tug1 group in comparison to the sh-NC group ($p < 0.05$). In addition, flow cytometry and Transwell assay were applied to examine the effects lncRNA Tug1 silencing on cell viability, apoptotic rate, and migration ability of PASMCs (Fig. 2B&C&D). The results demonstrated that the cell viability and migration ability of PASMCs were markedly decreased, while the apoptotic rate was increased in the sh-Tug1 group in comparison to the sh-NC group ($p < 0.05$). Western blot analysis was conducted to detect the protein expression of proliferation-related protein Ki-67, apoptosis-related protein Bax, migration-related proteins MMP-2, and MMP-9 (Fig. 2E). The results revealed that the protein expression of Bax in PASMCs was higher, but the protein expression of PCNA, Ki-67, MMP-2, MMP-9 proteins was lower in the sh-Tug1 group in comparison to the sh-NC group. All the aforementioned results supported that lncRNA Tug1 silencing could inhibit the proliferation and migration, while promoting the apoptosis of vascular PASMCs.

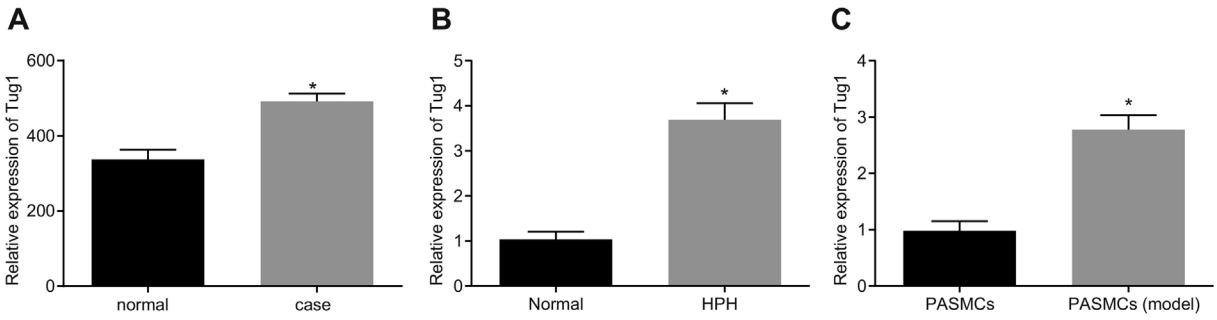

Fig. 1. High expression of lncRNA Tug1 is found in pulmonary artery smooth muscle tissues of HPH mice and HPH-PASMCs. A, expression of lncRNA Tug1 in the normal group (n = 6) and the case group (n = 6) in gene expression profile GSE2411. B, expression of lncRNA Tug1 in pulmonary artery smooth muscle tissues of HPH mice (n = 15) and normal pulmonary artery smooth muscle tissues of normal mice (n = 10) detected by RT-qPCR (*$p < 0.05$ *vs.* the normal group). C, expression of lncRNA Tug1 in normal PASMCs and HPH-PASMCs detected by RT-qPCR (*$p < 0.05$ *vs.* the PASMCs group). The values in the figure were all measurement data, which were expressed as mean ± standard deviation. Data comparisons between two groups were performed using the independent sample *t*-test from three independent experiments.

3.3. LncRNA Tug1 increases Foxc1 expression by competitively binding to miR-374c

LncRNA Tug1 localization was identified in PASMCs using RNA-FISH (Fig. 3A), which revealed that lncRNA Tug1 was primarily expressed in the cytoplasm of PASMCs. This indicated that lncRNA Tug1 might exhibit a potential regulatory function on miR-374c in PASMCs. Furthermore, the Starbase database (http://starbase.sysu.edu.cn/index.php) suggested that lncRNA Tug1 could bind to miR-374c. In addition, RT-qPCR results (Fig. 3B) demonstrated that miR-374c was down-regulated in both HPH-PASMCs and pulmonary artery smooth muscle tissues of HPH mice ($p < 0.05$). Moreover, pulmonary artery smooth muscle tissues were extracted from 15 mice to analyze the correlation between lncRNA Tug1 and miR-374c expression in tissues (Fig. 3C). It was found that a negative correlation existed between lncRNA Tug1 and miR-374c expression. Additionally, the Starbase website (http://starbase.sysu.edu.cn/index.php) showed that miR-374c could bind to Foxc1. Subsequently, lncRNA Tug1 was determined to be positively correlated with Foxc1 in pulmonary artery smooth muscle tissues of HPH mice (Fig. 3D). Additionally, RT-qPCR results displayed up-regulated expression of Foxc1 in PASMCs and pulmonary artery smooth muscle tissues of HPH mice (Fig. 3E). Thereafter, we investigated the effect of miR-374 on Foxc1 under HPH conditions. It was found that miR-374 negatively regulated the expression of Foxc1 (Fig. 3F). The bioinformatics website predicted that there were potential binding sites between lncRNA Tug1 and miR-374c, miR-374c and Foxc1 (Fig. 3G). Following the prediction, we measured the fluorescence intensity using dual luciferase reporter gene assay after co-transfection of mimic NC and miR-374c mimic with wt-Tug1, mut-Tug1, wt-Foxc1-3′UTR, and mut-Foxc1-3′UTR (Fig. 3H). It was found that in comparison to the mimic NC group, co-transfection between miR-374c mimic and wt-Tug1 or wt-Foxc1-3′UTR resulted in a significant decrease in fluorescence intensity ($p < 0.05$), whereas no evident differences were detected in fluorescence intensity after co-transfection between miR-374c mimic and mut-Tug1 or mut-Foxc1-3′UTR ($p > 0.05$). Furthermore, RIP assay showed that the enrichment abundance of miR-374c, lncRNA Tug1 and Foxc1 mRNA in the anti-Ago2 group was all significantly increased in comparison to the anti-IgG group ($p < 0.05$) (Fig. 3I). Ultimately, Ago2 could bind to lncRNA Tug1, miR-374c and Foxc1. Therefore, the results confirmed that lncRNA Tug1 regulated Foxc1 expression by competitively binding to miR-374c.

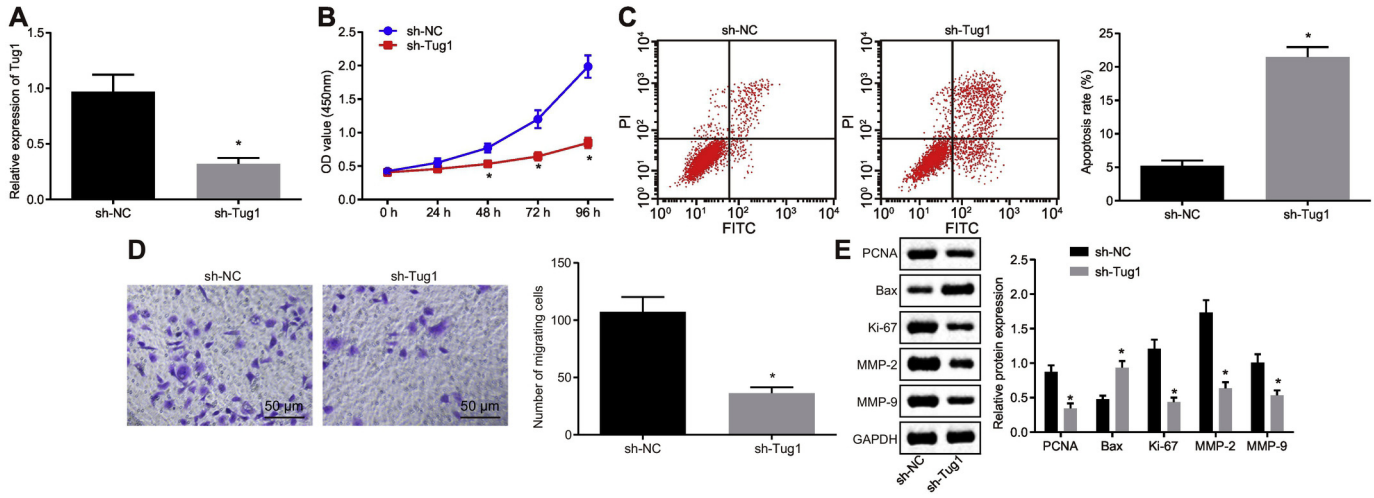

Fig. 2. The proliferation and migration of HPH-PASMCs are inhibited, while apoptosis is promoted by silencing lncRNA Tug1. A, silencing efficiency in PASMCs treated with sh-NC and sh-Tug1. B, PASMC viability following silencing lncRNA Tug1 examined by CCK-8 assay. C, the effect of lncRNA Tug1 silencing on the apoptosis rate of PASMCs assessed by flow cytometry. D, the effect of lncRNA Tug1 silencing on migration ability of PASMCs measured by Transwell assay (×200). E, relative protein expression of proliferation-related protein Ki-67, apoptosis-related protein Bax and migration-related proteins MMP-2 and MMP-9 in PASMCs after silencing lncRNA Tug1 evaluated by Western blot analysis (*$p < 0.05$ *vs.* the sh-NC group). The values in the figure were all measurement data, which were expressed as mean ± standard error. Data comparisons between two groups were performed using the independent sample *t*-test, and repeated measures ANOVA was used for data comparison at different time points. Cell experiments were repeated three times to obtain the mean value.

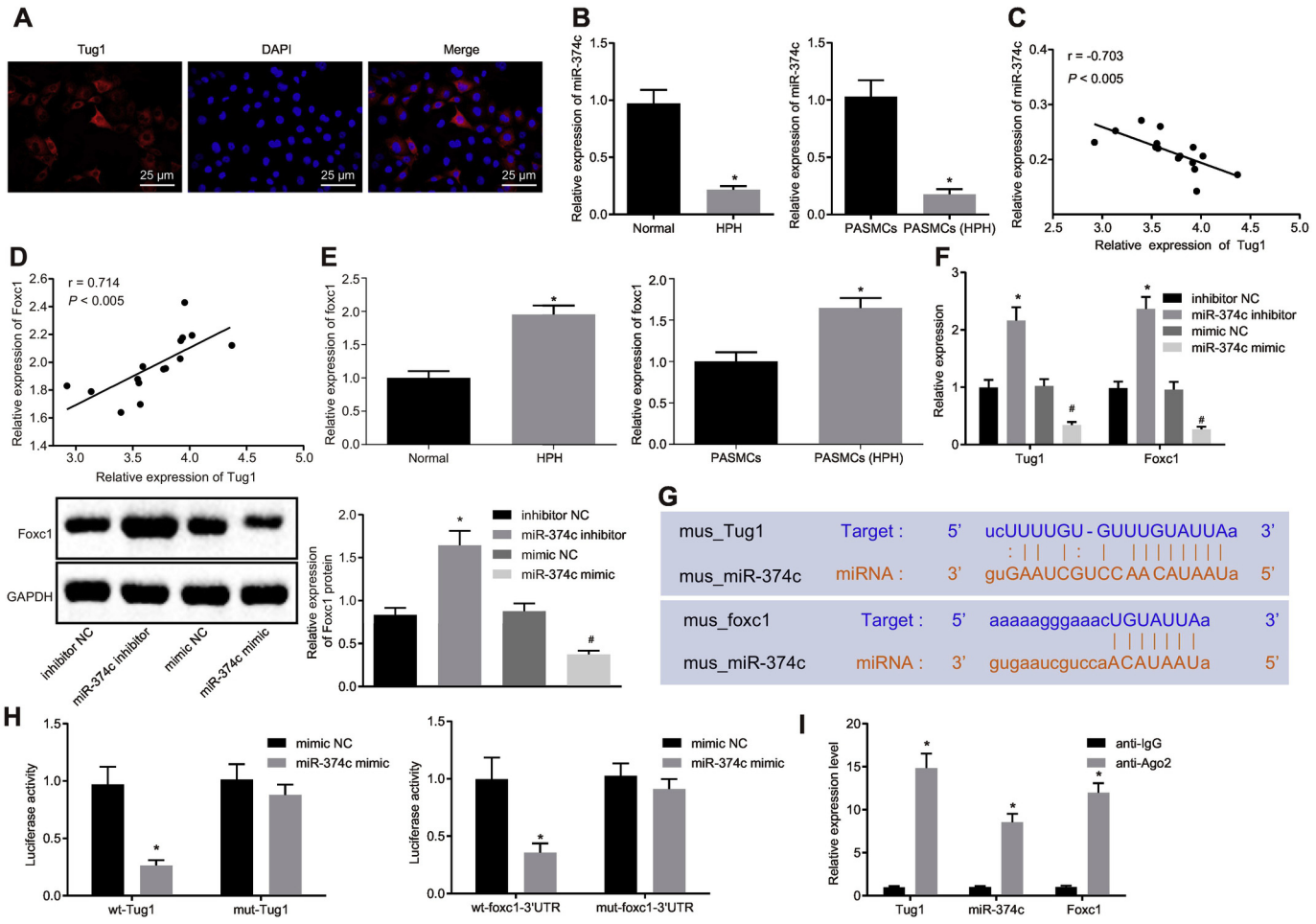

Fig. 3. LncRNA Tug1 up-regulates the expression of Foxc1 by competitively binding to miR-374c. A, the localization of lncRNA Tug1 in PASMCs identified by RNA-FISH (×400). B, expression of miR-374c in pulmonary artery smooth muscle tissues of mice (10 normal mice and 15 HPH mice) and PASMCs measured by RT-qPCR (*$p < 0.05$ *vs.* the normal mice or the normal PASMCs). C, correlation between the expression of lncRNA Tug1 and miR-374c in tissues analyzed by Pearson correlation analysis (n = 15). D, correlation between the expression of lncRNA Tug1 and Foxc1 in pulmonary artery smooth muscle tissues of HPH mice analyzed by Pearson correlation analysis (n = 15). E, expression of Foxc1 under normoxic and hypoxic conditions. F, expression of lncRNA Tug1 and Foxc1 in cells treated with silenced or over-expressed miR-374c (*$p < 0.05$ *vs.* the inhibitor NC group; $^{\#}p < 0.05$ *vs.* the mimic NC group). G, the potential binding site of miR-374c to lncRNA Tug1 and Foxc1 predicted by bioinformatics website. H, the fluorescence intensity after mimic NC and miR-374c mimic co-transfected with wt-Tug1, mut-Tug1, wt-Foxc1-3′UTR, and mut-Foxc1-3′UTR respectively detected by dual luciferase reporter assay (*$p < 0.05$ *vs.* the mimic NC group). E. I, the binding of Ago2 to lncRNA Tug1, miR-374c or Foxc1 detected by RIP assay (*$p < 0.05$ *vs.* the anti-IgG group). The values in the figure were all measurement data, which were expressed as mean ± standard error. Data comparisons between two groups were performed using the independent sample *t*-test and the comparison among multi-groups was analyzed by one-way ANOVA, followed by Tukey's *post hoc* test. Cell experiments were repeated three times to obtain the mean value.

3.4. LncRNA Tug1 silencing inhibits proliferation and migration, while promoting apoptosis of hypoxic vascular PASMCs by regulating Foxc1 expression

Several previous studies have revealed that Foxc1 activates the NOTCH signaling pathway [18], and the activation promotes pulmonary vascular remodeling in HPH [14]. Furthermore, it has been confirmed that lncRNA Tug1 could regulate Foxc1 expression *via* mediating miR-374c. Therefore, our focus shifted to determine whether the effects of lncRNA Tug1 on the biological characteristics of PASMCs could be achieved by regulating Foxc1 and binding to miR-374c under normoxic and hypoxic conditions.

RT-qPCR was employed to detect the transfection efficiency of PASMCs under hypoxic condition (Fig. 4A). The results displayed that lncRNA Tug1 expression and mRNA expression of Foxc1 were significantly decreased in the sh-Tug1 + oe-NC group compared to the sh-NC + oe-NC group. However, the expression of lncRNA Tug1 was notably decreased, while the mRNA expression of Foxc1 gene was significantly increased in the sh-Tug1 + oe-Foxc1 group; the mRNA expression of Foxc1 in the sh-NC + oe-Foxc1 group was also significantly elevated ($p < 0.05$). Additionally, cell viability, apoptosis rate, and migration ability of PASMCs under normoxic or hypoxic conditions were assessed using CCK-8 assay, flow cytometry, and Transwell assay, respectively (Fig. 4B&C&D). The results revealed that cell viability (under hypoxic conditions) and migration ability of PASMCs were reduced, whereas the apoptosis rate was markedly elevated from the 48th h onwards in the sh-Tug1 + oe-NC group relative to the sh-NC + oe-NC group. In addition, the sh-NC + oe-Foxc1 group presented with opposite trends ($p < 0.05$). In comparison with the sh-Tug1 + oe-NC group, cell viability (under hypoxic conditions) and migration ability of PASMCs were significantly decreased, while the apoptosis rate increased from the 48th h in the sh-Tug1 + oe-Foxc1 group ($p < 0.05$). Results of the Western blot analysis, which was applied to determine the protein expression of Ki-67, Bax, MMP-2 and MMP-9 (Fig. 4E), demonstrated that in comparison to the sh-NC + oe-NC group, the protein expression of Bax was increased, while that of PCNA, Ki-67, MMP-2 and MMP-9 was decreased in PASMCs in the sh-Tug1 + oe-NC group. Opposite trends were observed in terms of the

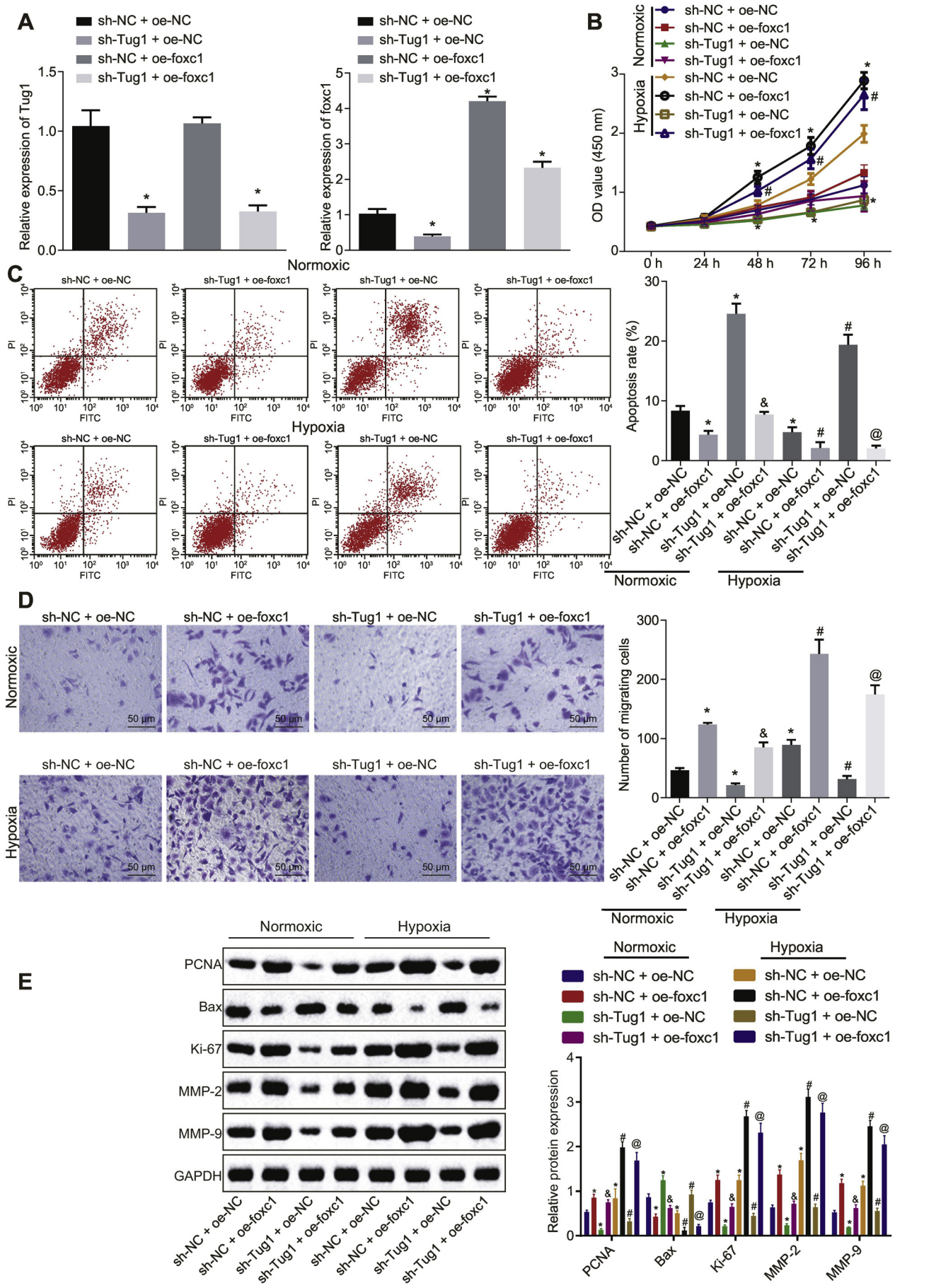

(caption on next page)

Fig. 4. LncRNA Tug1 silencing suppresses proliferation and migration, but promotes the apoptosis of HPH-PASMCs by down-regulating the expression of Foxc1. The PASMCs used for following assays were treated with both sh-NC and oe-NC, both sh-NC and oe-Foxc1, both sh-Tug1 and oe-NC, as well as both sh-Tug1 and oe-Foxc1. A, the expression of lncRNA Tug1 and Foxc1 in PASMCs after different treatments (*$p < 0.05$ *vs.* the oe-NC + sh-NC group under hypoxic condition). B, the viability of PASMCs after different treatments detected by CCK-8 assay (*$p < 0.05$ *vs.* the oe-NC + sh-NC group under hypoxic condition, $^{\#}p < 0.05$ *vs.* the sh-Tug1 + oe-NC group under hypoxic condition). C, the apoptosis rate of PASMCs after different treatments measured by flow cytometry. D, the Emigration ability of PASMCs after different treatments assessed by Transwell assay (×200). E, protein expression of proliferation-related protein Ki-67, apoptosis-related protein Bax and migration-related proteins MMP-2 and MMP-9 in PASMCs after different treatments detected by Western blot analysis (panels C–E: *$p < 0.05$ *vs.* the oe-NC + sh-NC group under normoxic condition, $^{\&}p < 0.05$ *vs.* the sh-Tug1 + oe-NC group under normoxic condition, $^{\#}p < 0.05$ *vs.* the oe-NC + sh-NC group under hypoxic condition, $^{@}p < 0.05$ *vs.* the sh-Tug1 + oe-NC group under hypoxic condition). The values in the figure were all measurement data, which were expressed as mean ± standard error. Data comparisons among multi-groups were analyzed by one-way ANOVA and repeated measures ANOVA was applied for comparison among multiple groups at different time points, followed by Tukey's *post hoc* test. Cell experiments were repeated three times to obtain the mean value.

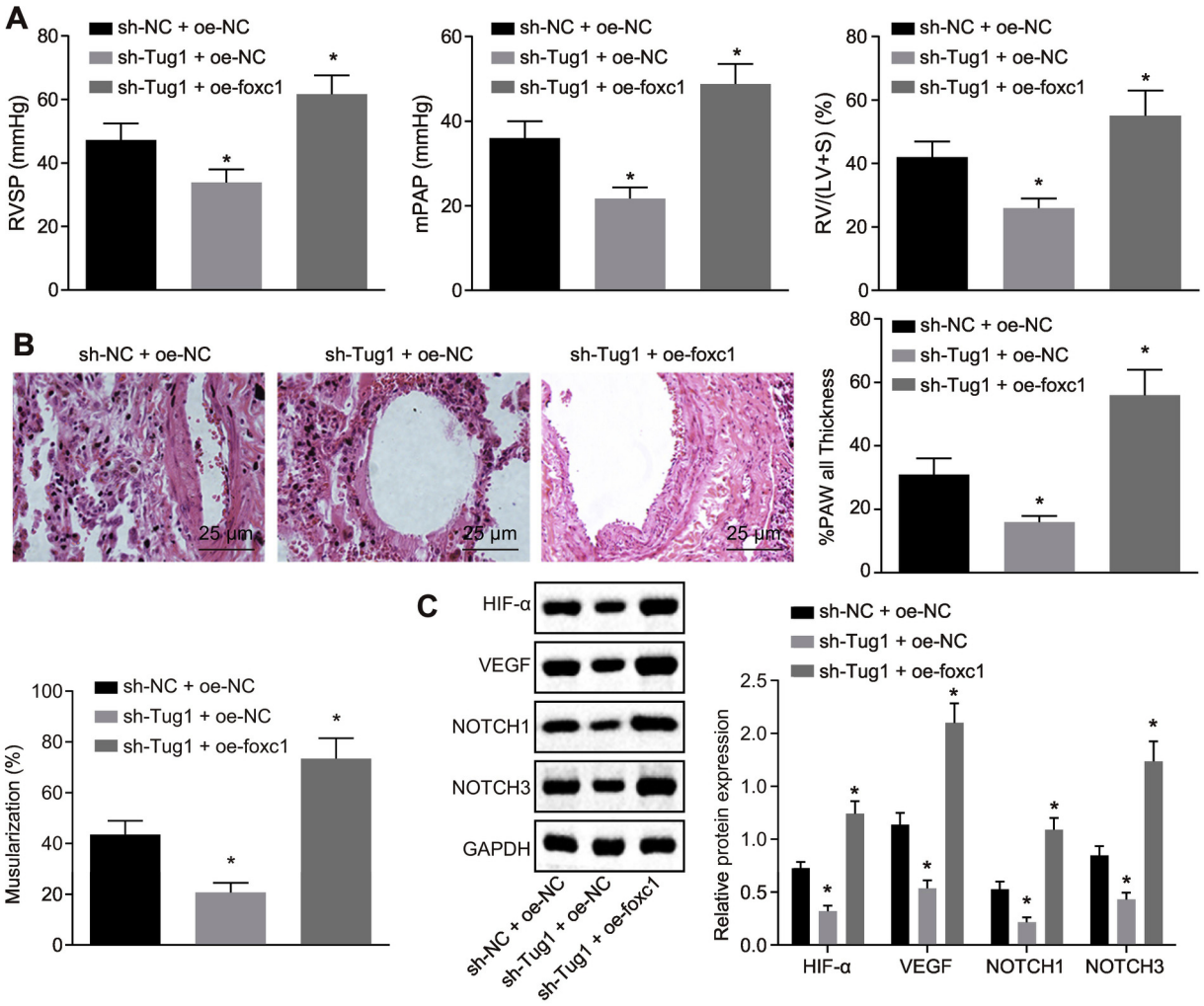

Fig. 5. Involvement of lncRNA Tug1/Foxc1/NOTCH signaling pathway in pulmonary vascular remodeling in HPH mice. The mice used for following assays were injected with cells after transfection with both sh-NC and oe-NC, both sh-Tug1 and oe-NC, as well as both sh-Tug1 and oe-Foxc1. A, blood pressure changes in mice. B, the tissues morphology, wall thickness of pulmonary artery wall (PAW) and muscularization of mice detected by HE staining (×400, scale bar = 25 μm). C, protein expression of HIF-α, VEGF, NOTCH1 and NOTCH3 in the mouse issues assessed by Western blot analysis (*$p < 0.05$ *vs.* the oe-NC + sh-NC group). The values in the figure were all measurement data, which were expressed as mean ± standard deviation. Data comparisons among multi-groups were analyzed by one-way ANOVA, followed by Tukey's *post hoc* test. Cell experiments were repeated three times to obtain the mean value, n = 5.

protein expression of the aforementioned factors in the sh-NC + oe-Foxc1 group ($p < 0.05$). Finally, the sh-Tug1 + oe-Foxc1 group exhibited an increased protein expression of Bax, but reduced protein expression of PCNA, Ki-67, MMP-,2 and MMP-9 in PASMCs in comparison to the sh-Tug1 + oe-NC group ($p < 0.05$). The above-mentioned results demonstrated that the proliferation and migration were suppressed, but apoptosis was promoted in PASMCs by down-regulation of lncRNA Tug1 *via* regulating Foxc1 expression.

3.5. LncRNA Tug1 participates in pulmonary vascular remodeling in HPH mice through the NOTCH signaling pathway via Foxc1 regulation

Next, we characterized the functional relevance of Foxc1-mediated activation of the Notch signaling pathway with lncRNA Tug1 and its role in pulmonary vascular remodeling in HPH mice.

Blood pressure measurement results (Fig. 5A) demonstrated that the RVSP, mPAP and wet weight ratio of RV to LV + s were all decreased in the sh-Tug1 + oe-NC group relative to the sh-NC + oe-NC group ($p < 0.05$), while opposite trends were observed in the sh-Tug1 + oe-

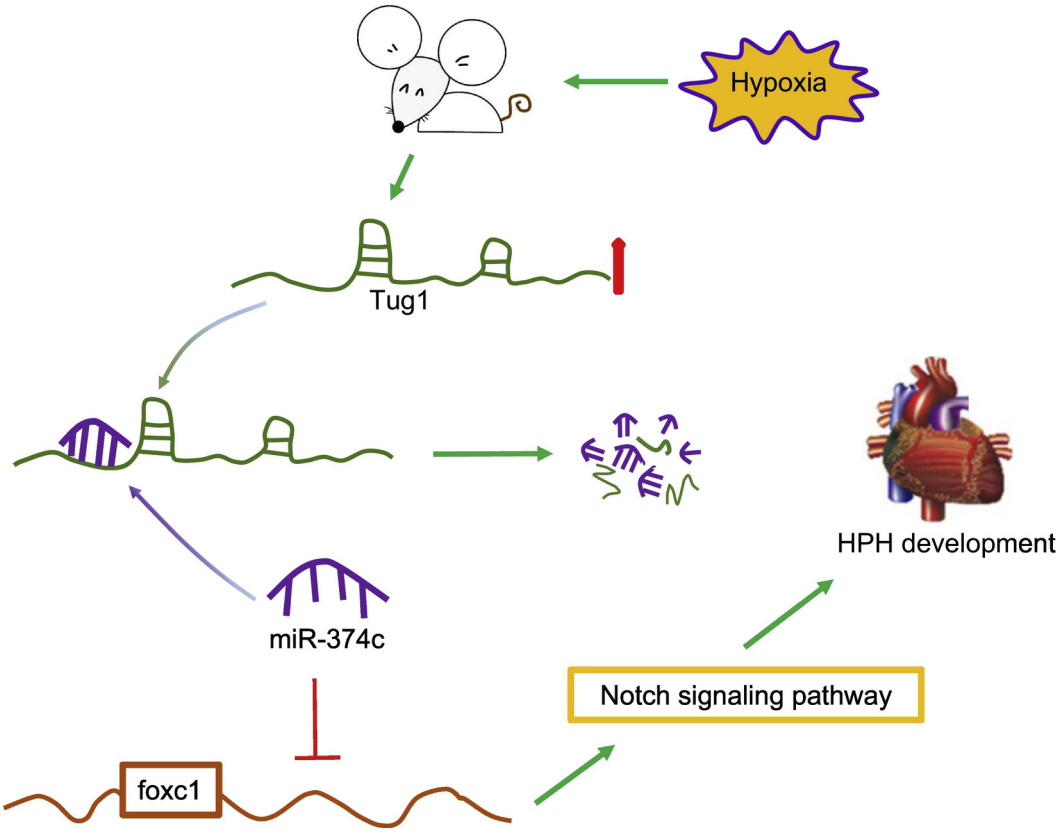

Fig. 6. The schematic diagram depicting the regulatory role of the lncRNA Tug1/miR-374c/Foxc1 axis implicated in the pulmonary vascular remodeling of HPH. Under hypoxic conditions, lncRNA Tug1 was highly-expressed and acted as a miR-374c sponge to up-regulate Foxc1 expression, thereby contributing to pulmonary vascular remodeling in HPH development through the Notch signaling pathway.

Foxc1 group ($p < 0.05$). HE staining results (Fig. 5B) revealed that the amount of arterial intima-stained blue particles was increased, while the PAW became thinner ($p < 0.05$), and muscularization was decreased in the sh-Tug1 + oe-NC group. Meanwhile, the sh-Tug1 + oe-Foxc1 group exhibited fewer arterial intima-stained blue particles, thicker PAW ($p < 0.05$), and increased muscularization in comparison with the sh-NC + oe-NC group. The results of Western blot analysis (Fig. 5C) illustrated that in comparison to the sh-NC + oe-NC group, the expression of HIF-α, VEGF, NOTCH1, and NOTCH3 was all lower in the sh-Tug1 + oe-NC group ($p < 0.05$), while it was higher in the sh-Tug1 + oe-Foxc1 group ($p < 0.05$). The results demonstrated that lncRNA Tug1 could act on NOTCH signaling pathway to participate in pulmonary vascular remodeling by regulating Foxc1.

4. Discussion

Multiple lncRNAs have been implicated in the pathogenesis of HPH, such as lncRNA MEG3 [19] and lncRNA TCONS_00034812 [20]. The results obtained from the present study revealed elevated expression of lncRNA Tug1 in HPH mouse models and PASMCs in hypoxia. Moreover, lncRNA Tug1 was demonstrated to participate in the pulmonary vascular remodeling of HPH by modulating PASMC proliferation, migration, and invasion by serving as a miR-374c sponge to positively modulate the expression of Foxc1.

Firstly, the current study provided evidence that lncRNA Tug1 and Foxc1 were up-regulated, while miR-374c was down-regulated in both HPH mice and hypoxic PASMCs. LncRNA Tug1 has been demonstrated to function as an oncogene or a tumor suppressor, with similar actions depending on specific biological processes [21]. Moreover, elevated TUG1 expression has been previously indicated to serve as a predictive influencer of unsatisfactory clinical outcomes in upper esophageal cancer [22]. Overexpressed lncRNA Tug1 contributes to a larger infarction volume in ischemic mice and an elevated apoptosis rate in oxygen-glucose deprived SH-SY5Y cells [23]. Thus, more studies should be focused on examining the contradictory role of lncRNA Tug1 on cellular proliferation. Interestingly, miR-374 has also been reported to exhibit a contradictory role on cellular proliferation. For instance, in the validation cohort in multivariate analyses, forced expression of hsa-miR-374c was previously observed to improve recurrence-free survival of adenoid cystic carcinoma [24]. Moreover, miR-374 enhances proliferation and migration of transformed mesenchymal stem cells *via* regulation of the Wnt5a/beta-catenin signaling pathway [25]. We obtained opposite results in the PASMCs in our findings, which might be ascribed to the distinct cell types that miR-374 worked on. Additionally, miR-374 exerts a cardioprotective role by inhibiting dystrobrevin alph (DTNA)-controlled NOTCH1 expression in myocardial ischemia-reperfusion injury [26]. This suggests that miR-374 is an environment indicator to regulate the physiological function of the cardiovascular system. Therefore, these results strongly indicated the heavy involvement of lncRNA Tug1 and miR-374 in HPH.

Additionally, the current study also demonstrated that knockdown of lncRNA Tug1 led to significant decreases in proliferation, migration and invasion of PASMCs, while increasing apoptosis by modulating the miR-374c/Foxc1 axis, as reflected by reduced expression of PCNA, Ki-67, MMP-2, and MMP-9 as well as enhanced Bax. Likewise, down-regulated lncRNA Tug1 exerts an inhibitory effect over the expression of MMP-2 and MMP-9 in human pancreatic cancer [27]. Furthermore, Xu et al. demonstrated that the MMP-2 and MMP-9 are simultaneously diminished following Foxc1 reduction in primary hepatocellular carcinoma cell, also highlighting the major role of Foxc1 in enhancement of migration and invasion [28]. These findings illustrated the contribution of the lncRNA Tug1/miR-374c/Foxc1 axis in PASMC functions in HPH.

Another significant finding of our study was that the lncRNA Tug1/miR-374c/Foxc1/NOTCH axis could regulate the expression of HIF-α and VEGF, thereby modulating pulmonary vascular remodeling. By directly controlling the recruitment of human T cells to vessels, VEGF contributes to vascular remodeling in human arteries, thus opening a wider window for novel therapeutic targets for vascular remodeling on the basis of VEGF suppression [29]. Moreover, another study verified that lncRNA Tug1 up-regulates the expression of VEGF by binding to miR-34a, which in turn promotes tumor angiogenesis [30]. Also, VEGF-receptor1 has been verified to be a target gene of miR-374 and is up-regulated in ET-1-treated cardiomyocytes, probably as a consequence of the decline of miR-374 expression during the onset of myocardial hypertrophy [31]. Notably, loss of HIF-2α is also known to significantly attenuate pulmonary vascular remodeling is in mice [32]. In Drosophila blood cells, the association between NOTCH and HIF-α is essential for cell development and survival [33]. Moreover, it has also been indicated that Foxc1 could potentially activate the Notch signaling pathway, further promoting pulmonary vascular remodeling in HPH [16]. All these findings shed light on the influence of lncRNA Tug1/miR-374c/Foxc1/NOTCH axis on cytokines in blood to regulate HPH.

Overall, the current study illustrated the regulatory role of lncRNA Tug1 in pulmonary vascular remodeling of HPH. LncRNA Tug1 acts as a miR-374c sponge to accelerate pulmonary vascular remodeling in HPH by facilitating the migration and invasion of PASMCs and diminishing their apoptosis by up-regulating Foxc1 expression (Fig. 6). Hence, the lncRNA Tug1/miR-374c/Foxc1 network could be regarded as a potential target for the HPH therapies based on attenuating pulmonary vascular remodeling in the future. However, it should be noted that the state of hypoxia may be different by establishing the HPH mouse models through hypoxia for different time periods, which is a limitation of our study and requires further research.

Supplementary data to this article can be found online at https://doi.org/10.1016/j.lfs.2019.116769.

Funding source

None.

Acknowledgments

We would like to express our gratitude for the helpful comments provided by the reviewers.

Declaration of competing interest

The authors have no competing interests to declare.

Author contributions

Lei Yang and Huan Liang designed the study. Li Shen and Zhanjiang Guan collated the data, carried out data analyses and produced the initial draft of the manuscript. Xianguo Meng contributed to drafting the manuscript. All authors have read and approved the final submitted manuscript.

References

[1] A. Frost, D. Badesch, J.S.R. Gibbs, et al., Diagnosis of pulmonary hypertension, Eur. Respir. J. 53 (1) (2019).
[2] N. Galie, M. Humbert, J.L. Vachiery, et al., 2015 ESC/ERS guidelines for the diagnosis and treatment of pulmonary hypertension: the Joint Task Force for the Diagnosis and Treatment of Pulmonary Hypertension of the European Society of Cardiology (ESC) and the European Respiratory Society (ERS): endorsed by: Association for European Paediatric and Congenital Cardiology (AEPC), International Society for Heart and Lung Transplantation (ISHLT), Eur. Heart J. 37 (1) (2016) 67–119.
[3] E. Cahill, S.C. Rowan, M. Sands, et al., The pathophysiological basis of chronic hypoxic pulmonary hypertension in the mouse: vasoconstrictor and structural mechanisms contribute equally, Exp. Physiol. 97 (6) (2012) 796–806.
[4] L.A. Shimoda, S.S. Laurie, Vascular remodeling in pulmonary hypertension, J. Mol. Med. (Berl) 91 (3) (2013) 297–309.
[5] K.R. Stenmark, K.A. Fagan, M.G. Frid, Hypoxia-induced pulmonary vascular remodeling: cellular and molecular mechanisms, Circ. Res. 99 (7) (2006) 675–691.
[6] S. Mizuno, H.J. Bogaard, D. Kraskauskas, et al., p53 gene deficiency promotes hypoxia-induced pulmonary hypertension and vascular remodeling in mice, Am. J. Physiol. Lung Cell. Mol. Physiol. 300 (5) (2011) L753–L761.
[7] R.A. McDonald, A. Hata, M.R. MacLean, et al., MicroRNA and vascular remodelling in acute vascular injury and pulmonary vascular remodelling, Cardiovasc. Res. 93 (4) (2012) 594–604.
[8] J.S. Mattick, J.L. Rinn, Discovery and annotation of long noncoding RNAs, Nat. Struct. Mol. Biol. 22 (1) (2015) 5–7.
[9] B. Han, P. Bu, X. Meng, et al., Microarray profiling of long non-coding RNAs associated with idiopathic pulmonary arterial hypertension, Exp. Ther. Med. 13 (6) (2017) 2657–2666.
[10] L. Guo, Z. Qiu, L. Wei, et al., The microRNA-328 regulates hypoxic pulmonary hypertension by targeting at insulin growth factor 1 receptor and L-type calcium channel-alpha1C, Hypertension 59 (5) (2012) 1006–1013.
[11] Z. Li, J. Shen, M.T. Chan, et al., TUG1: a pivotal oncogenic long non-coding RNA of human cancers, Cell Prolif. 49 (4) (2016) 471–475.
[12] Y. Huang, H. Huang, M. Li, et al., MicroRNA-374c-5p regulates the invasion and migration of cervical cancer by acting on the Foxc1/snail pathway, Biomed. Pharmacother. 94 (2017) 1038–1047.
[13] H.Y. Koo, T. Kume, FoxC1-dependent regulation of vascular endothelial growth factor signaling in corneal avascularity, Trends Cardiovasc. Med. 23 (1) (2013) 1–4.
[14] Q. Guo, H. Xu, X. Yang, et al., Notch activation of Ca(2+)-sensing receptor mediates hypoxia-induced pulmonary hypertension, Hypertens. Res. 40 (2) (2017) 117–129.
[15] R. Du, W. Sun, L. Xia, et al., Hypoxia-induced down-regulation of microRNA-34a promotes EMT by targeting the Notch signaling pathway in tubular epithelial cells, PLoS One 7 (2) (2012) e30771.
[16] L. Jing, Y. Jia, J. Lu, et al., MicroRNA-9 promotes differentiation of mouse bone mesenchymal stem cells into neurons by Notch signaling, Neuroreport 22 (5) (2011) 206–211.
[17] R. Zhao, Q. Yan, H. Huang, et al., Transdermal siRNA-TGFbeta1-337 patch for hypertrophic scar treatment, Matrix Biol. 32 (5) (2013) 265–276.
[18] C.Y. Hwang, IY Kim, KS Kwon. Nucleocytoplasmic translocation and ubiquitin-dependent degradation of p21Cip1 by reactive oxygen species, FASEB J, 21, 2007, Meeting Report.
[19] B. Zhu, Y. Gong, G. Yan, et al., Down-regulation of lncRNA MEG3 promotes hypoxia-induced human pulmonary artery smooth muscle cell proliferation and migration *via* repressing PTEN by sponging miR-21, Biochem. Biophys. Res. Commun. 495 (3) (2018) 2125–2132.
[20] Y. Liu, Z. Sun, J. Zhu, et al., LncRNA-TCONS_00034812 in cell proliferation and apoptosis of pulmonary artery smooth muscle cells and its mechanism, J. Cell. Physiol. 233 (6) (2018) 4801–4814.
[21] H. Cai, X. Liu, J. Zheng, et al., Long non-coding RNA taurine upregulated 1 enhances tumor-induced angiogenesis through inhibiting microRNA-299 in human glioblastoma, Oncogene 36 (3) (2017) 318–331.
[22] Y. Xu, J. Wang, M. Qiu, et al., Upregulation of the long noncoding RNA TUG1 promotes proliferation and migration of esophageal squamous cell carcinoma, Tumour Biol. 36 (3) (2015) 1643–1651.
[23] M.H. Bao, V. Szeto, B.B. Yang, et al., Long non-coding RNAs in ischemic stroke, Cell Death Dis. 9 (3) (2018) 281.
[24] S. Andreasen, Q. Tan, T.K. Agander, et al., MicroRNA dysregulation in adenoid cystic carcinoma of the salivary gland in relation to prognosis and gene fusion status: a cohort study, Virchows Arch. 473 (3) (2018) 329–340.
[25] Z. Sun, J. Chen, J. Zhang, et al., The role and mechanism of miR-374 regulating the malignant transformation of mesenchymal stem cells, Am. J. Transl. Res. 10 (10) (2018) 3224–3232.
[26] Z. Zhao, Y. Zhao, L. Ying-Chun, et al., Protective role of microRNA-374 against myocardial ischemia-reperfusion injury in mice following thoracic epidural anesthesia by downregulating dystrobrevin alpha-mediated Notch1 axis, J. Cell. Physiol. 234 (7) (2019) 10726–10740.
[27] Y. Lu, L. Tang, Z. Zhang, et al., Long noncoding RNA TUG1/miR-29c axis affects cell proliferation, invasion, and migration in human pancreatic cancer, Dis. Markers 2018 (2018) 6857042.
[28] Z.Y. Xu, S.M. Ding, L. Zhou, et al., FOXC1 contributes to microvascular invasion in primary hepatocellular carcinoma *via* regulating epithelial-mesenchymal transition, Int. J. Biol. Sci. 8 (8) (2012) 1130–1141.
[29] J. Zhang, T. Silva, T. Yarovinsky, et al., VEGF blockade inhibits lymphocyte recruitment and ameliorates immune-mediated vascular remodeling, Circ. Res. 107 (3) (2010) 408–417.
[30] R. Dong, G.B. Liu, B.H. Liu, et al., Targeting long non-coding RNA-TUG1 inhibits tumor growth and angiogenesis in hepatoblastoma, Cell Death Dis. 7 (6) (2016) e2278.
[31] J.S. Lee, D.W. Song, J.H. Park, et al., miR-374 promotes myocardial hypertrophy by negatively regulating vascular endothelial growth factor receptor-1 signaling, BMB Rep. 50 (4) (2017) 208–213.
[32] H. Abe, H. Semba, N. Takeda, The roles of hypoxia signaling in the pathogenesis of cardiovascular diseases, J. Atheroscler. Thromb. 24 (9) (2017) 884–894.
[33] T. Mukherjee, W.S. Kim, L. Mandal, et al., Interaction between Notch and Hif-alpha in development and survival of Drosophila blood cells, Science 332 (6034) (2011) 1210–1213.